

Chiral perturbation theory calculation for $pn \rightarrow d\pi\pi$ at threshold

B. Liu^{1,2}, V. Baru^{2,3}, J. Haidenbauer^{2,4} and C. Hanhart^{2,4}

¹*School of Science, Xian Jiaotong University, Xian 710049, China*

²*Institut für Kernphysik and Jülich Center for Hadron Physics,
Forschungszentrum Jülich, D-52425 Jülich, Germany*

³*Institute for Theoretical and Experimental Physics,
117218, B. Cheremushkinskaya 25, Moscow, Russia*

⁴*Institute for Advanced Simulation,
Forschungszentrum Jülich, D-52425 Jülich, Germany*

(Dated:)

Abstract

We investigate the reaction $pn \rightarrow d\pi\pi$ in the framework of Chiral Perturbation Theory. For the first time a complete calculation of the leading order contributions is presented. We identify various diagrams that are of equal importance as compared to those recognized in earlier works. The diagrams at leading order behave as expected by the power counting. Also for the first time the nucleon–nucleon interaction in the initial, intermediate and final state is included consistently and found to be very important. This study provides a theoretical basis for a controlled evaluation of the non–resonant contributions in two–pion production reactions in nucleon–nucleon collisions.

I. INTRODUCTION

As the first strong inelastic threshold of the nucleon–nucleon system, pion production in NN collisions has attracted a large number of theoretical as well as experimental works. Due to advances in the experimental methods measurements in the threshold region became possible in the beginning of the 1990ies, and it quickly became clear that the theoretical models existing at the time [1] were not able to describe these data — see Ref. [2] and references therein. They fell short by a factor of two for reactions with an isoscalar NN pair in the final state, while there was a discrepancy of even more than an order of magnitude for those with an isovector NN pair in the final state. The numerous efforts to improve the phenomenological approaches [3, 4], although quite successful for various observables [5], did lack for systematics, gave contradictory answers, and involved a sensitivity to unobservable short range effects.

To overcome those deficiencies, in recent years considerable theoretical efforts went into the development of an effective field theory that can be applied to the reactions $NN \rightarrow NN\pi$. In early studies it became clear, however, that the original power counting by Weinberg [6, 7] needs modifications in order to arrive at a convergent expansion [8, 9] (see also Ref. [10] where it was pointed out that the naive power counting using the heavy baryon formalism is not applicable above the pion production threshold — the necessary adaptations are outlined in Ref. [11]). Indeed, for neutral pion production in pp collisions, the corrections due to the next-to-leading order (NLO) increased the discrepancy with the data and, moreover, the next-to-next-to-leading order (NNLO) contributions turned out to be even larger than the NLO terms [12]. The origin of these difficulties was identified quite early by Cohen et al. [13], see also [14], who stressed that the additional new scale, inherent in reactions of the type of $NN \rightarrow NN\pi$, needs to be accounted for in the power counting. Since the two nucleons in the initial state need to have sufficiently high kinetic energy to produce the on-shell pion in the final state, the initial center-of-mass momentum needs to be larger than

$$p_{\text{thr}}^{(1)} = \sqrt{M_N m_\pi}, \quad \text{with} \quad \frac{p_{\text{thr}}^{(1)}}{\Lambda_\chi} \simeq 0.4, \quad (1)$$

where m_π and M_N refer to the pion and nucleon mass, respectively, and Λ_χ denotes the typical hadronic scale, here identified with M_N to get a numerical estimate for the expansion parameter. The proper way to include this scale was presented in Ref. [15] and implemented

in Ref. [16], see Ref. [2] for a review article. As a result p -wave pion production is governed by tree-level diagrams up to NNLO [15, 17] in the modified power counting scheme. On the other hand, for s -wave pion production, pion loops, studied in detail in Ref. [18], start to contribute already at NLO. The individual loop contributions turned out to grow linearly with increasing NN relative momentum which resulted in a large sensitivity to the employed NN wave functions [19]. However, it was demonstrated in Refs. [18, 20] that all irreducible loop contributions at NLO cancel altogether which was needed to keep the scheme self-consistent. Furthermore, the proper separation of irreducible terms at NLO from reducible ones in the loops resulted in an increase of the most important LO operator for charged pion production, first investigated in Ref. [1], by a factor of 4/3. This increase was sufficient to overcome the apparent discrepancy with the data in the reaction $pp \rightarrow d\pi^+$. The neutral pion channel is more challenging — it still calls for a calculation of subleading loop contributions. First steps in this direction were taken in Refs. [11, 21]. We further emphasize that the $\Delta(1232)$ isobar should be taken into account explicitly as a dynamical degree of freedom [13] because the Delta-nucleon mass difference, ΔM , is also of the order of p_{thr} . This general argument was confirmed numerically in phenomenological calculations [5, 22, 23], see also Refs. [16, 20] where the effect of the Δ in $NN\pi$ was studied within ChPT.

The progress in the theory of isospin conserving pion production in nucleon-nucleon collisions allowed us to perform a complete leading-order calculation of charge symmetry breaking effects in $pn \rightarrow d\pi^0$ [24], see also Refs. [25, 26] for related works.

Given the developments just discussed, one now should be in the position to investigate two-pion production in NN collisions using the same formalism. Such calculations do not exist yet, although in the pioneering works of Refs. [27, 28] some constraints from chiral symmetry were already implemented. A more recent phenomenological analysis of this reaction can also be found in Ref. [29]. For two-pion production in NN collisions at threshold, the center-of-mass momentum of the initial nucleons is necessarily larger by a factor of $\sqrt{2}$ compared to the single-pion production. Thus we now have

$$p_{\text{thr}}^{(2)} = \sqrt{2m_\pi M_N} \approx 510 \text{ MeV} . \quad (2)$$

With this large momentum scale, the value of the expansion parameter is

$$\chi = \frac{p_{\text{thr}}^{(2)}}{M_N} \approx 0.54 \quad (3)$$

and one may question the applicability of ChPT for the two-pion production case. However, while the expansion may converge slowly, it is still meaningful at least close to the chiral limit and therefore should also provide some guideline on the hierarchy of diagrams. Thus it is still interesting and important to investigate the structure of diagrams that contribute at the lowest orders. Note that, since the NN momentum at the threshold for two-pion production is quite close to the one for single-pion production, for the purpose of power counting below we identify the two.

The amount of experimental data for $NN \rightarrow NN\pi\pi$ has increased greatly in recent years [30–33] and even a polarized measurement exists [34]. However, up to now there are no data available sufficiently close to threshold to allow for a straightforward comparison with our leading order calculation of the reaction $pn \rightarrow d\pi\pi$. To extend our calculation to higher energies the inclusion of the Δ as an explicit degree of freedom will be necessary (it enters at NLO). In addition, at NNLO, besides a large number of loops, also the first $NN \rightarrow NN\pi\pi$ counterterms start to contribute. The physics of those is dominated by heavier baryon resonances — most prominently the Roper resonance, as follows from previous phenomenological studies of the reactions $NN \rightarrow NN\pi\pi$ [27–29]. Two pion production and the role of the Roper resonance, in particular, has been studied extensively in the single-nucleon sector, namely in the reactions $\gamma N \rightarrow \pi\pi N$ and $\pi N \rightarrow \pi\pi N$ both phenomenologically, see, e.g., Refs. [35–38] and within ChPT [39–43]¹. In particular, ChPT studies [39, 40] predict that the double-neutral-pion photoproduction is significantly enhanced near threshold as compared to the production of the charged pions due to the contribution of chiral (pion) loops at NLO ($O(p^3)$). This prediction was confirmed experimentally in Ref. [44]. Also it was found in Ref. [39] that the Δ -isobar contribution, which is potentially important because the Δ -nucleon mass difference is of comparable magnitude to $2m_\pi$, turns out to be insignificant due to specific cancellations of the individual contributions. The Roper resonance contributes to this process at one order higher, i.e. at N²LO ($O(p^4)$). The effect of the Roper resonance encoded in low-energy constants was found to be sizable although significantly smaller than the contribution of the leading chiral loops [40]. Similar conclusions about the role of the Roper resonance were drawn based on studies of $\pi N \rightarrow \pi\pi N$. In this case, however, the loops were found to be negligible [42] and the

¹ Note that for the reaction $\pi N \rightarrow \pi\pi N$ within ChPT we refer to the calculations at order $O(p^3)$ only, see references cited in [39–43] for numerous other studies.

leading contribution was provided by tree level terms. For two-neutral-pion production in NN collisions we expect the production mechanism to be in accord with the dimensional analysis, i.e it should be dominated by the tree level graphs at LO. However, an explicit study of loops at NLO will be necessary to support our uncertainty estimates.

The paper is structured in the following way: In Sect. II our theoretical framework is introduced. Results for the reaction $pn \rightarrow d\pi^0\pi^0$ are presented and discussed in Sect. III. A summary and some concluding remarks are provided in Sect. IV. Technical details of our calculations are summarized in two Appendices.

II. THEORETICAL FORMALISM

Our calculations are based on the effective chiral Lagrangian [45–47]:

$$\begin{aligned}\mathcal{L}^{(0)} &= \frac{1}{2f_\pi^2}[(\boldsymbol{\pi} \cdot \partial_\mu \boldsymbol{\pi})^2 - \frac{1}{4}\boldsymbol{\pi}^2(\partial^\mu \boldsymbol{\pi})^2] + N^\dagger \frac{1}{4f_\pi^2} \boldsymbol{\tau} \cdot (\dot{\boldsymbol{\pi}} \times \boldsymbol{\pi}) N \\ &\quad + \frac{g_A}{2f_\pi} N^\dagger \boldsymbol{\tau} \cdot \vec{\sigma} \cdot \left(\vec{\nabla} \boldsymbol{\pi} + \frac{1}{2f_\pi^2} \boldsymbol{\pi}(\boldsymbol{\pi} \cdot \vec{\nabla} \boldsymbol{\pi}) \right) N + \dots \\ \mathcal{L}^{(1)} &= \frac{1}{8M_N f_\pi^2} \left(iN^\dagger \boldsymbol{\tau} \cdot (\boldsymbol{\pi} \times \vec{\nabla} \boldsymbol{\pi}) \cdot \vec{\nabla} N + h.c. \right) - \frac{g_A}{4M_N f_\pi} [iN^\dagger \boldsymbol{\tau} \cdot \dot{\boldsymbol{\pi}} \vec{\sigma} \cdot \vec{\nabla} N + h.c.] + \\ &\quad \frac{1}{f_\pi^2} N^\dagger \left[\left(c_2 + c_3 - \frac{g_A^2}{8M_N} \right) \dot{\boldsymbol{\pi}}^2 - c_3 (\vec{\nabla} \boldsymbol{\pi})^2 - 2c_1 m_\pi^2 \boldsymbol{\pi}^2 - \frac{1}{2} \left(c_4 + \frac{1}{4M_N} \right) \epsilon_{ijk} \epsilon_{abc} \sigma_k \tau_c \partial_i \pi_a \partial_j \pi_b \right] N \\ &\quad + \dots\end{aligned}\tag{4}$$

where the superscripts 0 and 1 denote the leading and next-to-leading order Lagrangian, respectively, f_π denotes the pion decay constant in the chiral limit, g_A is the axial-vector coupling of the nucleon, N and π are the nucleon and pion field, respectively, and $\vec{\sigma}$ ($\boldsymbol{\tau}$) denotes the Pauli matrix in spin (isospin) space. The ellipses in the above equations represent terms which are not relevant for the present study.

As mentioned in the Introduction, the system is characterized by three scales, where we use

$$m_\pi \ll p \sim p_{\text{thr}}^{(1)} \sim p_{\text{thr}}^{(2)} \sim \Delta M \ll \Lambda_\chi.$$

The counting rules here are similar to those for one-pion production used in [15–18] (for a review see also [2]). For the Weinberg-Tomozawa (WT) $\pi N \rightarrow \pi N$ vertex, as discussed in detail in Ref. [18], the leading term should be proportional to $2\omega_\pi$ where ω_π is the energy of the outgoing (on-shell) pion. The diagrams that contribute at the lowest order are shown in

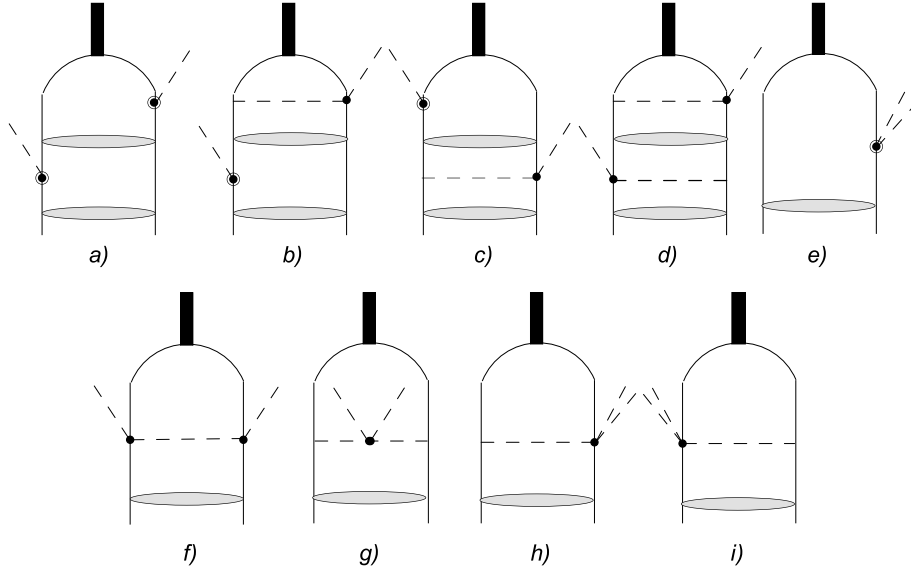


FIG. 1. Leading order diagrams for the reaction $pn \rightarrow d\pi\pi$ at threshold. Solid (dashed) lines denote nucleons (pions), filled ellipses correspond to continuum NN wave functions (including plane wave) in the initial and intermediate state, the outgoing black line denotes the deuteron. Subleading vertices are marked as \odot .

Fig. 1 and start to contribute at order $\chi \sim m_\pi/M_N$. Obviously, the number of diagrams is significantly larger for two-pion production than for one-pion production already at LO — after all the latter appears as building block of the former in diagrams a)–d). For Fig. 1d), we note that the naive dimensional analysis shows that this diagram contributes at next-to-leading order. However, due to the existence of the two-nucleon cut in the intermediate state, this diagram is promoted to leading order following the very same logic adopted by Weinberg [7]. In addition, Fig. 1 e)–i) show genuine two-pion production diagrams. Note that the only non-resonant diagrams included in the earlier studies of Refs. [27, 28] are those depicted in the second line of Fig. 1, whereas in Ref. [29] such diagrams are not considered at all.

Another potentially important class of contributions arises from diagrams where one of the nucleons is excited to the $\Delta(1232)$ -resonance. However, in the reaction considered here the $N\Delta$ system can only couple to the NN system in the intermediate state. The NN systems in the initial and final states have to have isospin zero, cf. below, while the $N\Delta$ system has always isospin one. The $\Delta(1232)$ can only appear when the first pion is emitted

and, thus, the power counting for the $\Delta(1232)$ in $pn \rightarrow d\pi\pi$ is similar to the one in single-pion production. In particular, the $\Delta(1232)$ starts to contribute at NLO due to the fact that the Δ propagator is suppressed by $1/p$ as compared to $1/m_\pi$ in the nucleon case. Moreover, the aforementioned isospin arguments prevent the potentially dangerous situation when there is an extremely enhanced Δ -propagator $(\Delta M - 2m_\pi - \text{recoil})^{-1}$ in the $N\Delta$ intermediate state that would occur from a Δ excitation prior to the first pion emission. It is interesting to note that a similar observation was made in Ref. [39] in the reaction $\gamma N \rightarrow \pi\pi N$ where the corresponding term $(\Delta M - 2m_\pi)^{-1}$ did not show up in the denominator because of an exact cancellation with the same term in the numerator.

Once the production operators are constructed, they should be convoluted with NN wave functions to account for the nonperturbative character of NN interaction [7]. In principle, the NN wave functions should be calculated on the same basis as the production operators. However, up to now ChPT NN interactions are only available for energies below the one-pion production threshold [48–50]. Therefore, in this work we adopt the so-called hybrid approach that consists in the convolution of the production operator calculated within ChPT with phenomenological NN wave functions from realistic NN models, in particular from the CCF model [51]. We utilize also wave functions generated from the CD-Bonn NN potential [52] so that we can examine in how far our results depend on the specific choice of the NN wave functions. The $\Delta(1232)$ resonance is included as explicit degree of freedom in the construction of the CCF potential [51] as well as in an extended version of the CD-Bonn potential [53]. This will allow us to extend in a future work the present calculation to higher orders in a straightforward manner. The ellipses in the Feynman diagrams of Fig. 1 refer to the NN wave functions and represent either the Initial State Interaction (ISI) or the Intermediate State Interaction (ImSI) of nucleon pairs supplemented with the plane wave terms.

Based on the Lagrangian given above, it is straightforward to calculate the amplitudes corresponding to the diagrams shown in Fig. 1. Furthermore, since we are only interested in the energy region very near to threshold, only a few partial waves contribute to the reaction amplitude. At threshold, the $\pi\pi$ system is in a relative S-wave and its isospin can be either zero or two as required by the symmetry of a system of identical bosons. However, since the isospin of the initial NN system can only be zero or one and the deuteron is an isosinglet the isospin of the produced $\pi\pi$ pair has to be zero and, consequently, also the isospin of the

TABLE I. The values of the amplitudes for the individual diagrams (in units of $10^{-2} \times \text{MeV}^{-1}$).

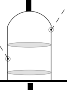
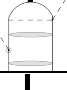
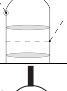
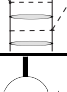
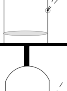
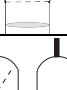
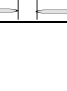
<p>1a)</p> $\mathcal{A}_{^3S_1} = 1.9 - i 0.9$ $\mathcal{A}_{^3D_1} = -3.9 + i 2.7$ <p>1b)</p> $\mathcal{A}_{^3S_1} = -6.5 + i 9.6$ $\mathcal{A}_{^3D_1} = 10.5 - i 5.0$ <p>1c)</p> $\mathcal{A}_{^3S_1} = 3.1 - i 0.8$ $\mathcal{A}_{^3D_1} = 0.6 + i 0.4$ <p>1d)</p> $\mathcal{A}_{^3S_1} = -7.1 + i 0.3$ $\mathcal{A}_{^3D_1} = -0.1 - i 2.9$	<p>1e)</p> $\mathcal{A}_{^3S_1} = -12.5 + i 3.1$ $\mathcal{A}_{^3D_1} = 6.6 - i 2.4$ <p>1f)</p> $\mathcal{A}_{^3S_1} = 2.3 - i 0.7$ $\mathcal{A}_{^3D_1} = -0.4 + i 0.6$ <p>1g) - i)</p> $\mathcal{A}_{^3S_1} = 1.6 - i 0.03$ $\mathcal{A}_{^3D_1} = 12.5 - i 7.2$
$\mathcal{A}_{full}^{^3S_1} = -17.2 + i 10.6$	$\mathcal{A}_{full}^{^3D_1} = 25.8 - i 13.8$

initial NN state is zero. Then the conservation of parity and angular momentum further requires that the total angular momentum of the system should be one and the NN pair in the initial state can only be in the 3S_1 or 3D_1 partial waves. The Pauli principle is also satisfied in this case. The explicit expressions for the amplitudes of these two partial waves can be found in Appendix A.

III. RESULTS AND DISCUSSION

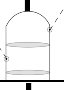
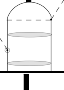
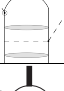
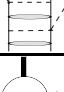
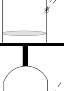

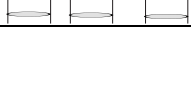
As discussed in the introduction, some leading order diagrams depicted in Figs. 1a)- 1e) are missing in Ref. [27]. First, we want to discuss the role of the diagrams 1a)- 1d). As

TABLE II. Values of the individual amplitudes for the 3S_1 partial wave (in $10^{-2} \times \text{MeV}^{-1}$).

	Born A_0	Initial state Interaction A_{ISI}		Intermediate state Interaction A_{ImSI}	Initial State Int. + Intermediate state Int. $A_{ISI+ImSI}$		sum
		${}^3S_1 \rightarrow {}^3S_1$	${}^3S_1 \rightarrow {}^3D_1$		${}^3S_1 \rightarrow {}^3S_1$	${}^3S_1 \rightarrow {}^3D_1$	
1a) 	11.6	$-3.4 - i2.8$	$-1.6 - i0.2$	$-7.8 + i0.1$	$2 + i1.9$	$1.1 + i0.1$	$1.9 - i0.9$
1b) 	-23.9	$4 + i7.3$	$3 + i$	$14 + i7.5$	$-1.8 - i5$	$-1.8 - i1.2$	$-6.5 + i9.6$
1c) 	$13.3 + i3.4$	$-5.5 - i3.5$	$1.5 + i0.2$	$-8.8 - i3.2$	$3.4 + i2.7$	$-0.8 - i0.4$	$3.1 - i0.8$
1d) 	$-22.7 - i14.5$	$7.5 + i10$	$-2.1 - i2$	$13 + i13$	$-3.7 - i7.5$	$0.9 + i1.3$	$-7.1 + i0.3$
1e) 	-14.4	$-6.2 + i3.4$	$8.1 - i0.3$	—	—	—	$-12.5 + i3.1$
1f) 	3.5	$-1.6 - i0.6$	$0.4 - i0.1$	—	—	—	$2.3 - i0.7$
1g)-i) 	-4.6	$2 + i0.6$	$4.2 - i0.6$	—	—	—	$1.6 - i0.03$

can be seen from the figure, these diagrams are closely related to the one-pion production case. There the leading order contributions come from the direct pion emission and the rescattering term. Thus, one may expect that the amplitudes 1a)- 1d) reveal a pattern similar to the one-pion production case. For example, one may guess that the amplitude of Fig. 1a) should be much smaller than the one of Fig. 1b) due to the fact that for single-pion production the rescattering term dominates over the direct one by an order of magnitude. However, it should be noted that in our case the NN amplitude in the intermediate state is fully off-shell and it turns out that the real part of diagram b) is larger only by a factor of about 3 as compared to the one of diagram a) — cf. Table I. In addition, due to the fact that the NN amplitudes for the ISI appear in coupled channels (3S_1 - 3D_1) the production amplitudes, as given in Table I, do not have the same phase. This fact makes the interference between the individual amplitudes very different from the one-pion production case and a direct comparison becomes difficult. The role of the NN interaction in the initial and intermediate states can be understood from looking at the individual contributions to the

TABLE III. Values of the individual amplitudes for the 3D_1 partial wave (in $10^{-2} \times \text{MeV}^{-1}$).

	Born A_0	Initial state Interaction A_{ISI}		Intermediate state Interaction A_{ImSI}	Initial State Int. + Intermediate state Int. $A_{ISI+ImSI}$		sum
		$^3D_1 \rightarrow ^3D_1$	$^3D_1 \rightarrow ^3S_1$		$^3D_1 \rightarrow ^3D_1$	$^3D_1 \rightarrow ^3S_1$	
1a) 	-8.2	$0.5 + i3.3$	$-2.4 + i0.4$	$5.5 - i0.1$	$-0.4 - i1.7$	$1.1 + i0.8$	$-3.9 + i2.7$
1b) 	16.9	$1.2 - i5.2$	$4.1 + i4.8$	$-9.9 - i5.3$	$-0.9 + i3.1$	$-0.9 - i2.4$	$10.5 - i5$
1c) 	$4.4 + i2.4$	$-1.5 - i1.9$	$-3.1 + i1.5$	$-1.7 - i2.3$	$0.5 + i1.1$	$2 - i0.4$	$0.6 + i0.4$
1d) 	$-3.8 - i10$	$-0.04 + i4$	$6.5 + i0.8$	$0.7 + i5.4$	$0.1 - i2.1$	$-3.6 - i$	$-0.1 - i2.9$
1e) 	37.9	$-5.1 - i19.4$	$-26.2 + i17$	—	—	—	$6.6 - i2.4$
1f) 	1.6	$-0.6 - i0.6$	$-1.4 + i1.2$	—	—	—	$-0.4 + i0.6$
1g)-i) 	17.9	$-5.1 - i7.1$	$-0.3 - i0.1$	—	—	—	$12.5 - i7.2$

two-pion production amplitudes listed in Tables II and III. We find that the values of these contributions are basically comparable with each other, as expected from the power counting. The values of the amplitudes of Fig. 1b) and Fig. 1d) are about a factor of two to three larger than the other two amplitudes 1a) and 1c), which is still a reflection of the dynamics governing the one-pion production. We observe that the resulting values of the amplitudes 1a)- 1d) are similar in size to those of 1f)- 1i) considered in previous studies [27, 28] and, thus, are important. We also find that the NN interaction in the initial and intermediate states plays an important role in the calculation, especially for the diagrams 1a)- 1d). In particular, one can find from Tables II and III that the inclusion of the NN interaction in the ISI or the ImSI generally reduces the magnitude of the amplitudes as compared to the Born amplitude and that the cancellation among the individual amplitudes of each particular diagram is significant. The largest cancellation takes place between the amplitudes with and without the ImSI, i.e. between $(\mathcal{A}_0$ and $\mathcal{A}_{ImSI})$ and $(\mathcal{A}_{ISI}$ and $\mathcal{A}_{ISI+ImSI})$ where the amplitudes are defined in Appendix A, see also Tables II and III. For example, the

value of the S-wave amplitude of Fig. 1a) becomes a factor of two smaller than the Born amplitude after including the ISI. When the ImSI is also considered, the full amplitude is further reduced so that it is finally a factor of six smaller than the Born amplitude. This observation shows explicitly that the ISI and the ImSI are very important quantitatively. Since they also strongly influence the phase of the amplitudes, their proper inclusion is compulsory, especially for studies of polarization observables.

The strength of the contact terms, that appear in Fig. 1e), is given by the low energy constants c_i that can be determined from πN scattering. Because we are only interested in the amplitudes at threshold, we only need the values of c_1 , c_2 and c_3 . In this work, we take the values from Ref. [54] where the values of c_i 's are obtained by fitting πN threshold parameters. To the order we are working, three solutions are offered in that paper. One corresponds to the results without considering the $\Delta(1232)$ explicitly, and the other two are results where the $\Delta(1232)$ is included but with different choices of the $\pi N \Delta$ coupling constant h_A . It is well known that c_2 and c_3 can be largely accounted for by the contribution from the $\Delta(1232)$ [55], and therefore the values of c_2 and c_3 can change significantly between extractions with and without inclusion of the $\Delta(1232)$. One may expect that using different sets of parameters will affect the value of the amplitudes of Fig. 1e) strongly. However, it is interesting to note that the amplitude of Fig. 1e) is independent of those choices, because it only depends on the value of the linear combination

$$2m_\pi^2 c_1 + q_1^0 q_2^0 (c_2 + c_3 - g_A^2/(8M_N)) , \quad (5)$$

with $q_1^0 = q_2^0 = m_\pi$ for the pion energies in the kinematics relevant here. From Table 1 of Ref. [54] one can see that the values of c_1 and $c_2 + c_3$ are not affected by the $\Delta(1232)$ up to order $O(p^2)$. Thus, although the values of c_2 and c_3 can significantly change individually by considering the $\Delta(1232)$ explicitly, the sum of them is not affected up to order $O(p^2)$, as shown explicitly in Ref. [55]. Hence at LO the contribution from contact terms are not influenced by the $\Delta(1232)$, which is also consistent with the power counting used. It is also interesting to note that the linear combination of low energy parameters displayed in Eq. (5) is large, for the individual terms interfere constructively — this is in contradistinction to πN scattering, where $q_1^0 = -q_2^0 = m_\pi$ holds at threshold and then physics is governed by the very small isoscalar scattering length [55], see Ref. [56] for a recent accurate extraction of a^+ from pionic atoms. Thus, once the reaction $pn \rightarrow d\pi^0\pi^0$ can be studied with sufficient

accuracy, it might be a good source of information for the c_i individually. Note also that in Ref. [54] the $1/M_N$ corrections are not included explicitly in the fits to πN data but absorbed effectively into the LECs c_i . To be consistent with their treatment we also drop the $1/M_N$ term in Eq. (5). Furthermore, the residual combination $c_2 + c_3$ which enters Eq. (5) is totally determined by the S -wave threshold parameters. Numerically the result for diagram 1e) turns out to be one of the largest individual contributions — cf. Table I.

The diagrams² of Figs. 1f)- 1i) are included in the previous study of Ref. [27], except for the initial state interaction which is not considered in that work. However, as can be seen from Tables II and III, the consistent inclusion of the ISI changes the value of the amplitudes 1f)- 1i) significantly and is thus important.

Besides the interference between the individual amplitudes of each particular diagram, the interference between the contributions from different diagrams is also very significant as can be seen from Tables II and III. In order to examine the sensitivity of our results and especially of the interference pattern to the employed NN interaction we also performed calculations with a different NN model, namely with the CD-Bonn model [52]. We found that the values of the individual amplitudes vary in a reasonable range (up to 30%) due to differences in the NN wave functions whereas the sum of all amplitudes varies just by a small amount (around 10%). This variation should be partly absorbed by the contribution of the $(N^\dagger N)^2 \pi\pi$ contact term at $N^2\text{LO}$.

To check the convergence of chiral expansions based on counting rules, it is necessary to calculate explicitly subleading contributions. As those calculations are not available yet, we may try to compare the results from the leading order contributions to experimental observables: our result should be within 50% of the data, given the relatively large value of the expansion parameter. The applicability of our s -wave calculation is restricted to the near-threshold regime and, therefore, data close to the threshold are needed for a sensible comparison of theory with experiment. Unfortunately, at present the empirical information for the $d\pi\pi$ channel is very scarce. Only data down to excess energies $Q = 70$ MeV ($Q = \sqrt{s} - \sqrt{s_{\text{thr}}}$) are available and the uncertainties are still very large. Thus, it is difficult to draw any conclusions about the convergence in the present work. In order to provide some comparison of our calculation with the existing data, we assume that the matrix element

² We checked, using the methods of Ref. [11], that the sum of the contributions from Figs. 1g)- 1i) is independent of the choice of the pion field, as required by field-theoretic consistency.

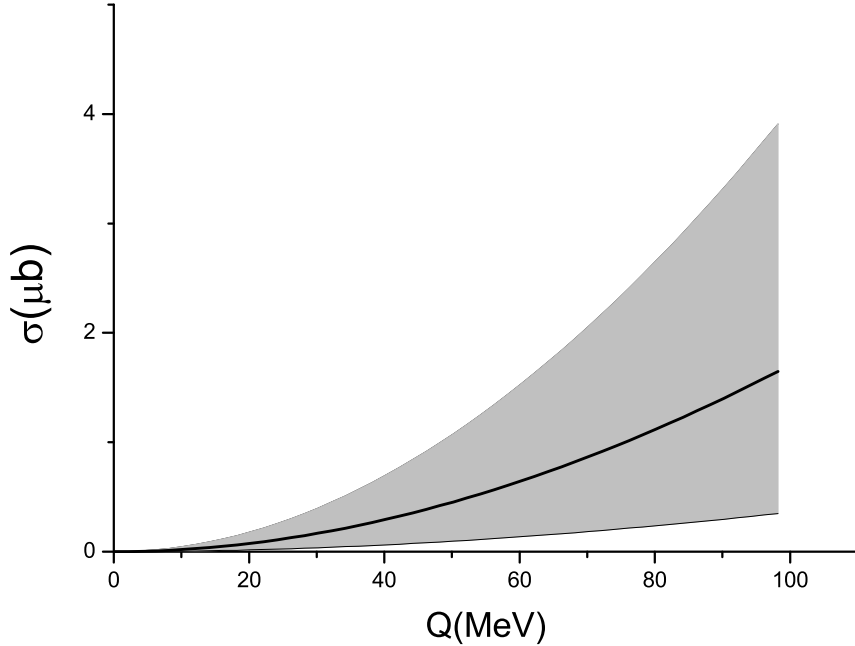


FIG. 2. Result of our ChPT calculation for the cross section of $pn \rightarrow d\pi^0\pi^0$ based on the assumption of a constant production amplitude. The shaded area corresponds to the uncertainty estimate based on a dimensional analysis.

is constant and therefore take the energy dependence as originating only from the three-body phase space. Our result is roughly a factor of two smaller than the central value of the data point at $Q = 70$ MeV. We want to stress, however, that the uncertainties of the experiment in question is quite large (even a factor of 25 larger than the data themselves). For future reference, in Fig. 2 we show the central value for the cross section predicted under the assumption that the matrix element is a constant and that no higher partial waves contribute. We also indicate the uncertainty band based on a dimensional analysis.

IV. SUMMARY

We presented a complete leading order calculation for the reaction $pn \rightarrow d\pi^0\pi^0$ at threshold within chiral perturbation theory. There is no free parameter in the calculation at this order. We included various additional diagrams as compared to previous investigations [27, 28]

and we also made several technical improvements. Our most important findings, summarized in Table I, are

- all diagrams evaluated are of similar importance;
- there are sizable interferences between the individual contributions;
- the accurate inclusion of the NN interaction in both intermediate as well as initial states is very important.

We also stress that for two-pion production the expansion parameter

$$\chi = \frac{p_{\text{thr}}^{(2)}}{M_N} \approx 0.54 ,$$

where $p_{\text{thr}}^{(2)}$ denotes the initial NN momentum at the two-pion production threshold, is rather large. It is therefore important to calculate higher order contributions to check the rate of convergence. We argue in this paper that despite of the proximity of the $\Delta(1232)$ to the $\pi\pi N$ threshold the potentially most important $N\Delta$ intermediate state is not allowed for the reaction $pn \rightarrow d\pi\pi$ because of isospin conservation. Intermediate states containing the $\Delta(1232)$ must be of the kind $\pi N\Delta$, i.e. can only occur after one-pion emission. Therefore, the role of the $\Delta(1232)$ resonance in the reaction considered is expected to be analogous to that in one-pion production. In particular, the $\Delta(1232)$ starts to contribute at next-to-leading order. Furthermore, it is known from phenomenological studies of $NN \rightarrow NN\pi\pi$ [27, 28] that the Roper resonance can play a significant role already near threshold and that it will become even more important when considering a larger range of energies. However, this resonance is not included explicitly in the present study. One may expect that its contribution is absorbed into some low energy constants. The contribution of the Roper resonance to the c_i parameters, that scale the strength of the leading isoscalar πN scattering, has been discussed, e.g., in Ref. [55]. It seems that it plays only a minor role here. Similar conclusions were drawn from systematic studies within ChPT of the double-pion photoproduction process [39, 40] and the reaction $\pi N \rightarrow \pi\pi N$ [41–43] near threshold. In particular, for the reaction $\gamma p \rightarrow \pi^0\pi^0 p$ the contribution of the Roper was found to be rather moderate as compared to the large contribution of chiral loops [40]. A recent model calculation of $\pi N \rightarrow \pi\pi N$ by S. Schneider et al. [35] suggests also that the Roper resonance plays a rather minor role. On the other hand, the Roper might contribute significantly to the $(N^\dagger N)^2\pi\pi$

counterterms, which enter at NNLO in a ChPT calculation of $NN \rightarrow NN\pi\pi$. Based on the discussions above, one can not expect that our current calculation can describe the experimental data well at higher energies. However, the presented calculation provides an estimate for the contribution of the non-resonant background near threshold. It therefore forms a basis for future studies and is thus a precondition to extract reliable information on the Roper resonance from near-threshold experiments.

ACKNOWLEDGMENTS

We thank U.-G. Meißner and H. Clement for useful comments. B.C.Liu acknowledges the supports from the Helmholtz-China Scholarship Council Exchange Program and the National Natural Science Foundation of China under Grants No. 10905046. This work was supported in parts by funds from the Helmholtz Association (grants VH-NG-222, VH-VI-231), by the DFG (grants SFB/TR 16 and 436 RUS 113/991/0-1), by the EU HadronPhysics2 project, and by the RFFI. The work of V.B. was supported by the State Corporation of the Russian Federation, “Rosatom”.

Appendix A: Reaction amplitudes

In this appendix, we present expressions for the amplitudes that we consider in this work. To obtain the partial wave amplitudes, we follow the technics developed in Ref. [57].

For the reaction $NN \rightarrow d\pi\pi$ at threshold, the initial state can only be in the 3S_1 or 3D_1 partial waves and the total isospin is zero. Thus, the amplitudes for $NN \rightarrow d\pi\pi$ at threshold can be written in the general form

$$\mathcal{M} = (\vec{\epsilon}^* \cdot \vec{\mathcal{S}}^{[3S_1]} \mathcal{A}_{full}^{3S_1} + \vec{\epsilon}^* \cdot \vec{\mathcal{S}}^{[3D_1]} \mathcal{A}_{full}^{3D_1}) \cdot (\vec{\pi} \cdot \vec{\pi}) \mathcal{I}_0, \quad (\text{A1})$$

where $\mathcal{S}_i^{[3S_1]} = \chi_2^T \sigma_2 \frac{\sigma_i}{\sqrt{2}} \chi_1$ and $\mathcal{S}_i^{[3D_1]} = \frac{3}{2}(\delta_{ij} - \frac{1}{3}\hat{n}_i\hat{n}_j) \cdot \chi_2^T \sigma_2 \sigma_j \chi_1$ denote the normalized spin-orbit structure of the initial nucleons for the 3S_1 and 3D_1 partial waves, respectively, $\mathcal{I}_0 = \varphi_2^T \frac{\tau_2}{\sqrt{2}} \varphi_1$ denotes the isospin structure of the initial states, $\mathcal{A}_{full}^{3S_1}$ and $\mathcal{A}_{full}^{3D_1}$ are the corresponding partial wave amplitudes, $\vec{\pi}$ is the isospin wave function of outgoing pions and $\vec{\epsilon}$ is the deuteron polarization vector. Here $\chi_1(\chi_2)$ and $\varphi_1(\varphi_2)$ are spinors of the initial nucleons in spin and isospin space, respectively, and \hat{n} denotes the unit vector of the relative momentum of the initial nucleons. The expressions for $\mathcal{A}_{full}^{3S_1(3D_1)}$ are obtained by projecting

the amplitudes that contribute to a given order into corresponding partial waves using the technics developed in Ref. [57]. To leading order, the relevant diagrams in our work are shown in Fig. 1. Each diagram in Fig. 1 represents a set of diagrams, in which possible NN interaction in the initial and intermediate NN states are considered. For example, the partial wave amplitudes of Figs. 1a)-d) originate from several parts as follows:

$$\mathcal{A}^{PW} = \mathcal{A}_0^{PW} + \mathcal{A}_{ISI}^{PW} + \mathcal{A}_{ImSI}^{PW} + \mathcal{A}_{ISI+ImSI}^{PW} , \quad (\text{A2})$$

where the index '0' stands for the Born diagram, and 'ISI', 'ImSI' or 'ISI+ImSI' correspond to the initial state interaction, intermediate state interaction, or both initial and intermediate state interactions included in the amplitudes, respectively. 'PW' represents the two possible partial waves in the initial state, which can be either 3S_1 or 3D_1 . For Figs. 1e)-i) the partial wave amplitudes contain only two parts, namely \mathcal{A}_0^{PW} and \mathcal{A}_{ISI}^{PW} because there is no intermediate state interaction.

To compute diagrams with the NN interaction in the initial and intermediate states we take the NN scattering amplitudes from some potential models. In our calculation, instead of the commonly used \mathcal{T} matrix, the \mathcal{M} matrix is used. These quantities are related by $\mathcal{M} = -8\pi^2 M_N^2 \mathcal{T}$. For the initial state interaction $\mathcal{M}_{NN}^{PW \rightarrow PW'}$ denotes the NN half-off-shell \mathcal{M} matrix, where $PW \rightarrow PW'$ represents the transition from the partial wave "PW" to "PW'" with "PW" and "PW'" being 3S_1 or 3D_1 in our case. For the intermediate state interaction, the only possible transition is $^3P_1 \rightarrow ^3P_1$, so we just use $\mathcal{M}_{NN}^{^3P_1 \rightarrow ^3P_1}$ to denote the fully off-shell NN \mathcal{M} matrix. For the deuteron-NN vertex we adopt the notation and structures used in Ref. [58]. We use $u(p)$ and $w(p)$ to denote the NN components of the deuteron wave function corresponding to S-wave and D-wave respectively. Clearly, the bound (deuteron) wave functions $u(p)$ and $w(p)$ should be calculated using the same potential model as the NN scattering amplitudes in the continuum state. In this work we use the CCF model [51] to generate the NN amplitudes and the deuteron wave functions. Since the $\Delta\Delta$ channel is considered in the CCF model, that can also couple to the deuteron, the NN part of the deuteron wave functions, $u(p)$ and $w(p)$, are normalized as:

$$\int \frac{d^3p}{(2\pi)^3} (u(p)^2 + w(p)^2) = 0.9864 . \quad (\text{A3})$$

In this work, we adopt the following values of the parameters: $f_\pi = 92.4$ MeV, $g_A = 1.32$, $m_\pi = 139.58$ MeV and $M_N = 938.27$ MeV. The loop integration is regularized using the

cut-off method with $p_{\text{cut}} = \Lambda_{\text{ChPT}} \approx 1 \text{ GeV}$. We checked that the dependence of the results on this parameter is small – the results change by 10% when Λ is increased to 10 GeV.

1. Amplitudes of Fig. 1 a)-d)

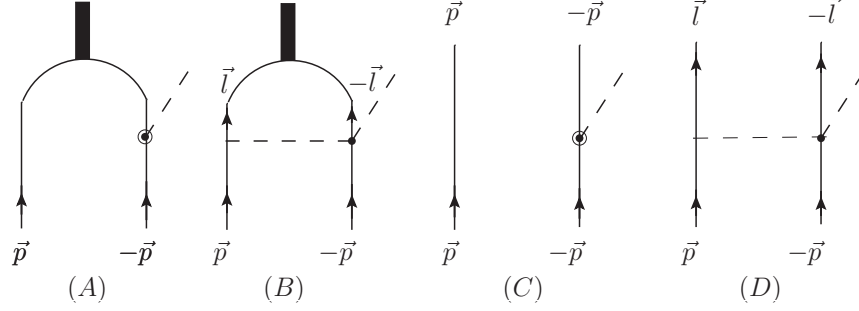


FIG. 3. Building blocks for construction the diagrams a)-d) of Fig. 1

To get the partial wave amplitudes of Fig. 1 a)-d) it is convenient to separate these diagrams into some building blocks at the position where the intermediate state interaction may occur, as shown in Fig. 3. Here the diagrams (A) and (B) correspond to the transition from the 3P_1 partial wave that is realized in the intermediate state in the diagrams of Fig. 1 a)-d) to the 3S_1 deuteron state. Correspondingly, the diagrams (C) and (D) represent the transition for the $^3S_1 - ^3D_1$ initial state of the two-nucleon pair to the intermediate 3P_1 state. The full amplitudes can then be obtained from the expressions for these building blocks by supplementing propagators, possible NN amplitudes and loop integrations. The amplitudes of Fig. 3(A) and (B) can be expressed in general as:

$$\mathcal{M} = (\vec{\epsilon}^* \cdot \vec{\mathcal{S}}^{[3P_1]} \vec{\mathcal{I}}_1 \cdot \vec{\pi}) \mathcal{B}, \quad (\text{A4})$$

where π_i is the isospin wave function of the π meson in the final state. Here we introduced $\mathcal{S}_i^{[3P_1]} = \frac{\sqrt{3}}{2} \epsilon_{ijk} \hat{p}_k \chi_2^T \sigma_2 \sigma_j \chi_1$ and $\mathcal{I}_{1,i} = \varphi_2^T \tau_2 \frac{\tau_i}{\sqrt{2}} \varphi_1$ to denote the normalized spin and isospin structures of the intermediate NN state, and $\hat{p} = \vec{p}/p$ is the unit vector of the relative NN momentum in the intermediate state. The expressions of \mathcal{B} for diagrams (A) and (B) are :

$$\begin{aligned} \mathcal{B}_A(p) &= -\sqrt{\frac{8}{3}} \frac{g_A m_\pi \sqrt{M_N}}{f_\pi} p \left(u(p) + \frac{w(p)}{2} \right), \\ \mathcal{B}_B(p) &= \frac{4}{\sqrt{3}} \frac{g_A m_\pi M_N^{\frac{3}{2}}}{f_\pi^3} \int \frac{l^2 dl}{2\pi^2} \int \frac{d\Omega_{\vec{p}}}{4\pi} \frac{d\Omega_{\vec{l}}}{4\pi} \frac{1}{(\vec{p} - \vec{l})^2 + m_\pi^2} \left(\frac{p}{4} (w(p) - \frac{u(p)}{\sqrt{2}}) \right) \end{aligned} \quad (\text{A5})$$

$$-\frac{3p}{4}w(p)(\hat{p} \cdot \hat{l})^2 + \frac{l}{\sqrt{2}}(u(p) + \frac{w(p)}{\sqrt{2}})\hat{p} \cdot \hat{l} \Big) . \quad (\text{A6})$$

Correspondingly, the expressions of the building blocks for Fig. 3(C) and (D) can be given in the following way:

$$\mathcal{M} = \left[(\vec{\mathcal{S}}^{\dagger 3S_1} \cdot \vec{\mathcal{S}}^{\dagger 3P_1}) \mathcal{B}^{3S_1} + (\vec{\mathcal{S}}^{\dagger 3D_1} \cdot \vec{\mathcal{S}}^{\dagger 3P_1}) \mathcal{B}^{3D_1} \right] \cdot (\vec{\mathcal{T}}_1^\dagger \cdot \vec{\pi}) \mathcal{I}_0 , \quad (\text{A7})$$

where \mathcal{B}^{3S_1} and \mathcal{B}^{3D_1} for the diagrams (C) and (D) read:

$$\mathcal{B}_C^{3S_1}(p) = \frac{p}{\sqrt{6}} \frac{g_A m_\pi}{M_N f_\pi} , \quad (\text{A8})$$

$$\mathcal{B}_C^{3D_1}(p) = -\frac{p}{2\sqrt{3}} \frac{g_A m_\pi}{M_N f_\pi} , \quad (\text{A9})$$

$$\mathcal{B}_D^{3S_1}(p, l) = -\frac{1}{\sqrt{6}} \frac{g_A m_\pi}{f_\pi^3} \int \frac{d\Omega_{\vec{p}}}{4\pi} \frac{d\Omega_{\vec{l}}}{4\pi} \frac{p\hat{p} \cdot \hat{l} - l}{(\vec{p} - \vec{l})^2 + m_\pi^2} , \quad (\text{A10})$$

$$\mathcal{B}_D^{3D_1}(p, l) = -\frac{\sqrt{3}}{4} \frac{g_A m_\pi}{f_\pi^3} \int \frac{d\Omega_{\vec{p}}}{4\pi} \frac{d\Omega_{\vec{l}}}{4\pi} \frac{l(\hat{p} \cdot \hat{l})^2 - \frac{2p}{3}\hat{p} \cdot \hat{l} - \frac{l}{3}}{(\vec{p} - \vec{l})^2 + m_\pi^2} . \quad (\text{A11})$$

Given the building blocks shown above and the corresponding NN scattering amplitudes, it is straightforward to construct the amplitudes of Fig. 1 a)-d). For example, the amplitudes corresponding to diagram 1a) are:

$$\mathcal{A}_0^{a,PW} = N_S \cdot \mathcal{B}_C^{PW}(p_i) \cdot \frac{M_N}{p_i^2 - p_1^2} \cdot \mathcal{B}_A(p_i) , \quad (\text{A12})$$

$$\begin{aligned} \mathcal{A}_{ISI}^{a,PW} = N_S \cdot \sum_{PW'}^{3S_1, 3D_1} \int \frac{p^2 dp}{2\pi^2} \frac{\mathcal{M}_{NN}^{PW \rightarrow PW'}(p_i, p)}{(2M_N)^2} \cdot \frac{M_N}{p^2 - p_2^2 - i\epsilon} \cdot \mathcal{B}_C^{PW'}(p) \\ \cdot \frac{M_N}{p^2 - p_1^2 - i\epsilon} \cdot \mathcal{B}_A(p) , \end{aligned} \quad (\text{A13})$$

$$\mathcal{A}_{ImSI}^{a,PW} = N_S \cdot \mathcal{B}_C^{PW}(p_i) \cdot \frac{M_N}{p_i^2 - p_1^2} \cdot \int \frac{l^2 dl}{2\pi^2} \frac{\mathcal{M}_{NN}^{3P_1 \rightarrow 3P_1}(p_i, l)}{(2M_N)^2} \cdot \frac{M_N}{l^2 - p_1^2 - i\epsilon} \cdot \mathcal{B}_A(l) , \quad (\text{A14})$$

$$\begin{aligned} \mathcal{A}_{ISI+ImSI}^{a,PW} = N_S \cdot \sum_{PW'}^{3S_1, 3D_1} \int \frac{p^2 dp}{2\pi^2} \frac{\mathcal{M}_{NN}^{PW \rightarrow PW'}(p_i, p)}{(2M_N)^2} \cdot \frac{M_N}{p^2 - p_2^2 - i\epsilon} \cdot \mathcal{B}_C^{PW'}(p) \cdot \frac{M_N}{p^2 - p_1^2 - i\epsilon} \\ \cdot \int \frac{l^2 dl}{2\pi^2} \frac{\mathcal{M}_{NN}^{3P_1 \rightarrow 3P_1}(p, l)}{(2M_N)^2} \cdot \frac{M_N}{l^2 - p_1^2 - i\epsilon} \cdot \mathcal{B}_A(l) , \end{aligned} \quad (\text{A15})$$

where $p_2 = p_{\text{thr}}^{(2)}$ and $p_1 = p_{\text{thr}}^{(1)}$. Here N_S is the symmetry factor which is obtained by considering the interchange of identical particles in the initial, intermediate and final states. This factor is the same as the number of Feynman diagrams one can get if we consider different ways to contract the operators in the initial, intermediate and final states. For diagrams 1a)-d) $N_s = 8 \cdot 2 \cdot \frac{1}{\sqrt{2}}$. Here 8 comes from the eight ways to contract the nucleon

field operators in the initial and intermediate states; 2 is to account the interchange of two identical pions in final states; $\frac{1}{\sqrt{2}}$ is from the deuteron vertex. It should be noted that in this way the possibility to produce pions from both nucleon lines is included. The corresponding expressions of Fig. 1b) can be obtained by changing \mathcal{C} to \mathcal{D} in the above equations.

The amplitudes of Figs. 1c) and 1d) can be obtained in a similar manner. The amplitudes of Fig. 1c) are

$$\mathcal{A}_0^{c,PW} = N_S \cdot \int \frac{l^2 dl}{2\pi^2} \mathcal{B}_D^{PW}(p_i, l) \cdot \frac{M_N}{l^2 - p_1^2 - i\epsilon} \cdot \mathcal{B}_A(l) , \quad (\text{A16})$$

$$\begin{aligned} \mathcal{A}_{ISI}^{c,PW} = N_S \cdot \sum_{PW'}^{^3S_1, ^3D_1} \int \frac{p^2 dp}{2\pi^2} \frac{\mathcal{M}_{NN}^{PW \rightarrow PW'}(p_i, p)}{(2M_N)^2} \cdot \frac{M_N}{p^2 - p_2^2 - i\epsilon} \cdot \int \frac{l^2 dl}{2\pi^2} \mathcal{B}_D^{PW'}(p) \\ \cdot \frac{M_N}{p^2 - p_1^2 - i\epsilon} \cdot \mathcal{B}_A(p) , \end{aligned} \quad (\text{A17})$$

$$\begin{aligned} \mathcal{A}_{ImSI}^{c,PW} = N_S \cdot \int \frac{l^2 dl}{2\pi^2} \mathcal{B}_D^{PW}(p_i, l) \cdot \frac{M_N}{l^2 - p_1^2 - i\epsilon} \cdot \int \frac{k^2 dk}{2\pi^2} \frac{\mathcal{M}_{NN}^{^3P_1 \rightarrow ^3P_1}(l, k)}{(2M_N)^2} \\ \cdot \frac{M_N}{k^2 - p_1^2 - i\epsilon} \cdot \mathcal{B}_A(k) , \end{aligned} \quad (\text{A18})$$

$$\begin{aligned} \mathcal{A}_{ISI+ImSI}^{c,PW} = N_S \cdot \sum_{PW'}^{^3S_1, ^3D_1} \int \frac{p^2 dp}{2\pi^2} \frac{\mathcal{M}_{NN}^{PW \rightarrow PW'}(p_i, p)}{(2M_N)^2} \cdot \frac{M_N}{p^2 - p_2^2 - i\epsilon} \cdot \int \frac{l^2 dl}{2\pi^2} \mathcal{B}_D^{PW'}(p, l) \cdot \frac{M_N}{p^2 - p_1^2 - i\epsilon} \\ \cdot \int \frac{k^2 dk}{2\pi^2} \frac{\mathcal{M}_{NN}^{^3P_1 \rightarrow ^3P_1}(l, k)}{(2M_N)^2} \cdot \frac{M_N}{l^2 - p_1^2 - i\epsilon} \cdot \mathcal{B}_A(k) . \end{aligned} \quad (\text{A19})$$

The corresponding amplitudes of Figs. 1d) can be obtained by changing A to B in the above equations.

2. Amplitudes of Fig. 1e)-h)

For the diagrams of Fig. 1e)-h) there is no intermediate state interaction so that the amplitude can be written as:

$$\mathcal{A}^{PW} = \mathcal{A}_0^{PW} + \mathcal{A}_{ISI}^{PW} . \quad (\text{A20})$$

Note that only the sum of the amplitudes of Figs. 1g)-i) is independent of the choice of the pion field. That is why below we give only the amplitude for the sum of them. The partial wave amplitudes of Figs. 1e)-i) without the ISI can be written as:

$$\mathcal{A}_0^{e, ^3S_1} = N_S^e \frac{4M_N^{\frac{3}{2}} m_\pi^2}{f_\pi^2} (-4c_1 - 2c_2 + \frac{g_A^2}{4M_N} - 2c_3) \cdot u(p) , \quad (\text{A21})$$

$$\mathcal{A}_0^{e,^3D_1} = -N_S^e \frac{4M_N^{\frac{3}{2}} m_\pi^2}{f_\pi^2} (-4c_1 - 2c_2 + \frac{g_A^2}{4M_N} - 2c_3) \cdot w(p), \quad (\text{A22})$$

$$\mathcal{A}_0^{f,^3S_1} = N_S^f \frac{2m_\pi^2 M_N^{\frac{3}{2}}}{f_\pi^4} \cdot \int \frac{l^2 dl}{2\pi^2} u(l) \cdot \int \frac{d\Omega_{\vec{p}}}{4\pi} \frac{d\Omega_{\vec{l}}}{4\pi} \frac{1}{(\vec{p} - \vec{l})^2 + m_\pi^2}, \quad (\text{A23})$$

$$\mathcal{A}_0^{f,^3D_1} = N_S^f \frac{m_\pi^2 M_N^{\frac{3}{2}}}{f_\pi^4} \cdot \int \frac{l^2 dl}{2\pi^2} w(l) \cdot \int \frac{d\Omega_{\vec{p}}}{4\pi} \frac{d\Omega_{\vec{l}}}{4\pi} \frac{1 - 3(\hat{p} \cdot \hat{l})^2}{(\vec{p} - \vec{l})^2 + m_\pi^2}, \quad (\text{A24})$$

$$\begin{aligned} \mathcal{A}_0^{g+h+i,^3S_1} &= N_S^{g+h+i} \frac{7\sqrt{2}g_A^2 M_N^{\frac{3}{2}} m_\pi^2}{3f_\pi^4} \int \frac{l^2 dl}{2\pi^2} \int \frac{d\Omega_{\vec{p}}}{4\pi} \frac{d\Omega_{\vec{l}}}{4\pi} \frac{1}{((\vec{p} - \vec{l})^2 + m_\pi^2)^2} \\ &\cdot \left[\left(w(l) - \frac{u(l)}{\sqrt{2}} \right) \cdot (\vec{p} - \vec{l})^2 - 3w(l) (p(\hat{p} \cdot \hat{l}) - l)^2 \right], \end{aligned} \quad (\text{A25})$$

$$\begin{aligned} \mathcal{A}_0^{g+h+i,^3D_1} &= N_S^{g+h+i} \frac{7g_A^2 M_N^{\frac{3}{2}} m_\pi^2}{3f_\pi^4} \int \frac{l^2 dl}{2\pi^2} \int \frac{d\Omega_{\vec{p}}}{4\pi} \frac{d\Omega_{\vec{l}}}{4\pi} \left[\frac{u(l)}{\sqrt{2}} \cdot (4p^2 - 8\vec{p} \cdot \vec{l} + 6l^2 (\hat{l} \cdot \hat{p})^2 - 2l^2) \right. \\ &\quad \left. + \frac{w(l)}{2} \cdot (p^2 - l^2 + 4\vec{p} \cdot \vec{l} - 3p^2 (\hat{p} \cdot \hat{l})^2 - 3l^2 (\hat{p} \cdot \hat{l})^2) \right] \\ &\cdot \frac{1}{((\vec{p} - \vec{l})^2 + m_\pi^2)^2}. \end{aligned} \quad (\text{A26})$$

The corresponding amplitudes with the ISI can be obtained through the following expression:

$$\mathcal{A}_{ISI}^{m,PW} = N_s^m \cdot \sum_{PW'}^{^3S_1,^3D_1} \int \frac{p^2 dp}{2\pi^2} \frac{\mathcal{M}_{NN}^{PW \rightarrow PW'}(p_i, p)}{(2M_N)^2} \cdot \frac{M_N}{p^2 - p_2^2 - i\epsilon} \cdot \mathcal{A}_0^{m, PW'}(p), \quad (\text{A27})$$

where m can be 'e', 'f', or 'g+h+i'. The symmetry factors for these amplitudes are $N_s^e = \frac{8}{\sqrt{2}}$, $N_s^f = \frac{4}{\sqrt{2}}$ and $N_s^{g+h+i} = \frac{4}{\sqrt{2}}$.

Appendix B: Observables

In this appendix we present the expressions for the cross section near threshold. The amplitudes of $pn \rightarrow d\pi\pi$ considered in this study are calculated at the threshold and, therefore, can be factored out of the phase space integration. The cross section for $pn \rightarrow d\pi^0\pi^0$ is expressed in terms of the amplitudes given in Appendix A in the following way:

$$\sigma = \frac{1}{4 \cdot 2 \cdot 2} \cdot (3|\mathcal{A}_{full}^{^3S_1}|^2 + 3|\mathcal{A}_{full}^{^3D_1}|^2) \cdot \frac{\Phi}{4E_{CM} p_{CM}} \quad (\text{B1})$$

where E_{CM} and p_{CM} are the energy and momentum of the initial nucleons in the c.m. frame. Φ is the phase space factor defined as:

$$\Phi = \int (2\pi)^4 \delta^4(P - p_{\pi_1} - p_{\pi_2} - p_d) \frac{d^3 p_{\pi_1}}{(2\pi)^3 2E_{\pi_1}} \frac{d^3 p_{\pi_2}}{(2\pi)^3 2E_{\pi_2}} \frac{d^3 p_d}{(2\pi)^3 2E_d} \quad (\text{B2})$$

The prefactor $\frac{1}{4 \cdot 2 \cdot 2}$ is due to averaging over the initial spin states, the isospin wave function of the initial NN states and the identity factor for the final pions, respectively. The factor of 3 in Eq. (B1) is from summing up the spin states.

-
- [1] D. S. Koltun and A. Reitan, Phys. Lett. **141** (1966) 1413.
 - [2] C. Hanhart, Phys. Rept. **397** (2004) 155 [arXiv:hep-ph/0311341].
 - [3] T. S. H. Lee and D. O. Riska, Phys. Rev. Lett. **70** (1993) 2237; C. J. Horowitz, H. O. Meyer and D. K. Griegel, Phys. Rev. C **49** (1994) 1337 [arXiv:nucl-th/9304004]; J. A. Niskanen, Phys. Rev. C **53** (1996) 526 [arXiv:nucl-th/9502015].
 - [4] E. Hernández and E. Oset, Phys. Lett. B **350** (1995) 158 [arXiv:nucl-th/9503019]; C. Hanhart, J. Haidenbauer, A. Reuber, C. Schütz and J. Speth, Phys. Lett. B **358** (1995) 21 [arXiv:nucl-th/9508005].
 - [5] C. Hanhart, J. Haidenbauer, O. Krehl and J. Speth, Phys. Rev. C **61** (2000) 064008 [arXiv:nucl-th/0002025].
 - [6] S. Weinberg, Phys. Lett. B **251** (1990) 288.
 - [7] S. Weinberg, Nucl. Phys. B **363** (1991) 3.
 - [8] B.Y. Park et al., Phys. Rev. C **53** (1996) 1519 [arXiv:nucl-th/9512023].
 - [9] C. Hanhart, J. Haidenbauer, M. Hoffmann, U.-G. Meißner and J. Speth, Phys. Lett. B **424** (1998) 8 [arXiv:nucl-th/9707029].
 - [10] V. Bernard, N. Kaiser and U.-G. Meißner, Eur. Phys. J. A **4** (1999) 259 [arXiv:nucl-th/9806013].
 - [11] C. Hanhart and A. Wirzba, Phys. Lett. B **650** (2007) 354 [arXiv:nucl-th/0703012];
 - [12] V. Dmitrašinović, K. Kubodera, F. Myhrer and T. Sato, Phys. Lett. B **465** (1999) 43 [arXiv:nucl-th/9902048]; S. I. Ando, T. S. Park and D. P. Min, Phys. Lett. B **509** (2001) 253 [arXiv:nucl-th/0003004].

- [13] T.D. Cohen, J.L. Friar, G.A. Miller and U. van Kolck, Phys. Rev. C **53** (1996) 2661 [arXiv:nucl-th/9512036].
- [14] C. da Rocha, G. Miller and U. van Kolck, Phys. Rev. C **61** (2000) 034613 [arXiv:nucl-th/9904031].
- [15] C. Hanhart, U. van Kolck, and G.A. Miller, Phys. Rev. Lett. **85** (2000) 2905 [arXiv:nucl-th/0004033].
- [16] C. Hanhart and N. Kaiser, Phys. Rev. C **66** (2002) 054005 [arXiv:nucl-th/0208050].
- [17] V. Baru, E. Epelbaum, J. Haidenbauer, C. Hanhart, A. E. Kudryavtsev, V. Lensky and U. -G. Meißner, Phys. Rev. C **80** (2009) 044003 [arXiv:0907.3911 [nucl-th]].
- [18] V. Lensky, V. Baru, J. Haidenbauer, C. Hanhart, A. E. Kudryavtsev and U.-G. Meißner, Eur. Phys. J. A **27** (2006) 37 [arXiv:nucl-th/0511054].
- [19] A. Gårdestig, D. R. Phillips and C. Elster, Phys. Rev. C **73** (2006) 024002 [arXiv:nucl-th/0511042].
- [20] V. Baru, J. Haidenbauer, C. Hanhart, A. E. Kudryavtsev, V. Lensky and U.-G. Meißner, *Proceedings of the 11th International Conference on Meson-Nucleon Physics and the Structure of the Nucleon (MENU 2007)*, Jülich, Germany, Sept. 10-14, 2007, p. 128 [arXiv:0711.2748 [nucl-th]].
- [21] Y. Kim, T. Sato, F. Myhrer and K. Kubodera, Phys. Rev. C **80** (2009) 015206 [arXiv:0810.2774 [nucl-th]].
- [22] J. A. Niskanen, Nucl. Phys. A **298** (1978) 417.
- [23] C. Hanhart, J. Haidenbauer, O. Krehl and J. Speth, Phys. Lett. B **444** (1998) 25 [arXiv:nucl-th/9808020].
- [24] A. Filin, V. Baru, E. Epelbaum, J. Haidenbauer, C. Hanhart, A. E. Kudryavtsev and U.-G. Meißner, Phys. Lett. B **681** (2009) 423 [arXiv:0907.4671 [nucl-th]].
- [25] D. R. Bolton and G. A. Miller, Phys. Rev. C **81** (2010) 014001 [arXiv:0907.0254 [nucl-th]].
- [26] U. van Kolck, J. A. Niskanen and G. A. Miller, Phys. Lett. B **493** (2000) 65 [arXiv:nucl-th/0006042].
- [27] L. Alvarez-Ruso, E. Oset and E. Hernández, Nucl. Phys. A **633** (1998) 519 [arXiv:nucl-th/9706046].
- [28] L. Alvarez-Ruso, Phys. Lett. B **452** (1999) 207 [arXiv:nucl-th/9811058].
- [29] X. Cao, B. S. Zou and H. S. Xu, arXiv:1004.0140 [nucl-th].

- [30] F. Kren *et al.* [CELSIUS/WASA Collaboration], Phys. Lett. B **684** (2010) 110 [arXiv:0910.0995 [nucl-ex]].
- [31] M. Bashkanov *et al.*, Phys. Rev. Lett. **102** (2009) 052301 [arXiv:0806.4942 [nucl-ex]].
- [32] T. Skorodko *et al.*, Phys. Lett. B **679** (2009) 30 [arXiv:0906.3087 [nucl-ex]].
- [33] J. Johanson *et al.*, Nucl. Phys. A **712** (2002) 75, and references therein.
- [34] S. Abd El-Bary *et al.* [COSY-TOF Collaboration], Eur. Phys. J. A **37** (2008) 267. [arXiv:0806.3870 [nucl-ex]].
- [35] S. Schneider, S. Krewald and U.-G. Meißner, Eur. Phys. J. A **28** (2006) 107.
- [36] H. Kamano, B. Juliá-Díaz, T. S. Lee, A. Matsuyama and T. Sato, Phys. Rev. C **80** (2009) 065203 [arXiv:0909.1129 [nucl-th]].
- [37] H. Kamano, B. Juliá-Díaz, T. S. Lee, A. Matsuyama and T. Sato, Phys. Rev. C **79** (2009) 025206 [arXiv:0807.2273 [nucl-th]].
- [38] J. A. Gómez Tejedor and E. Oset, Nucl. Phys. A **600** (1996) 413 [arXiv:hep-ph/9506209].
- [39] V. Bernard, N. Kaiser, U.-G. Meißner and A. Schmidt, Nucl. Phys. A **580** (1994) 474 [arXiv:nucl-th/9403013].
- [40] V. Bernard, N. Kaiser and U.-G. Meißner, Phys. Lett. B **382** (1996) 19 [arXiv:nucl-th/9604010].
- [41] V. Bernard, N. Kaiser and U.-G. Meißner, Nucl. Phys. B **457** (1995) 147 [arXiv:hep-ph/9507418].
- [42] N. Fettes, V. Bernard and U.-G. Meißner, Nucl. Phys. A **669** (2000) 269 [arXiv:hep-ph/9907276].
- [43] N. Mobed, J. Zhang and D. Singh, Phys. Rev. C **72** (2005) 045204.
- [44] M. Kotulla *et al.*, Phys. Lett. B **578** (2004) 63 [arXiv:nucl-ex/0310031].
- [45] C. Ordóñez and U. van Kolck, Phys. Lett. B **291** (1992) 459; U. van Kolck, U.T. Ph.D. (1993); C. Ordóñez, L. Ray, and U. van Kolck, Phys. Rev. Lett. **72** (1994) 1982; Phys. Rev. C **53** (1996) 2086.
- [46] V. Bernard, N. Kaiser and U.-G. Meißner, Int. J. Mod. Phys. E **4** (1995) 193 [arXiv:hep-ph/9501384].
- [47] V. Bernard, Prog. Part. Nucl. Phys. **60** (2008) 82 [arXiv:0706.0312 [hep-ph]].
- [48] P. F. Bedaque and U. van Kolck, Ann. Rev. Nucl. Part. Sci. **52** (2002) 339 [arXiv:nucl-th/0203055].

- [49] E. Epelbaum, Prog. Part. Nucl. Phys. **57** (2006) 654 [arXiv:nucl-th/0509032].
- [50] E. Epelbaum, H.-W. Hammer and U.-G. Meißner, Rev. Mod. Phys. **81** (2009) 1773 [arXiv:0811.1338 [nucl-th]].
- [51] J. Haidenbauer, K. Holinde and M. B. Johnson, Phys. Rev. C **48** (1993) 2190.
- [52] R. Machleidt, Phys. Rev. C **63** (2001) 024001.
- [53] A. Deltuva, R. Machleidt, and P. U. Sauer, Phys. Rev. C **68** (2003) 024005; A. Deltuva, private communication.
- [54] H. Krebs, E. Epelbaum and U.-G. Meißner, Eur. Phys. J. A **32** (2007) 127.
- [55] V. Bernard, N. Kaiser and U.-G. Meißner, Nucl. Phys. A **615** (1997) 483.
- [56] V. Baru, C. Hanhart, M. Hoferichter, B. Kubis, A. Nogga and D. R. Phillips, arXiv:1003.4444 [nucl-th].
- [57] V. Lensky, PhD Thesis, University of Bonn (2007).
- [58] V. Tarasov, V. Baru and A. Kudryavtsev, Phys. At. Nucl. **63** (2000) 801.